A Versatile Iris Segmentation Algorithm

P. Radu, K. Sirlantzis, G. Howells, S. Hoque, F. Deravi

School of Engineering and Digital Arts
University of Kent
Canterbury
United Kingdom
pr95@kent.ac.uk

Abstract: In biometric authentication, iris recognition was shown to be one of the most accurate techniques. In unconstrained environment and capture conditions (e.g. with hand-held devices used outdoors), the iris image may be contaminated by noise and distortions which makes the iris segmentation and recognition process difficult. This paper presents a novel iris segmentation algorithm that addresses some of the issues raised by unconstrained iris recognition. There are two main contributions in the present work: first, the proposed segmentation algorithm is able to cope efficiently with both near infra red and visible spectrum images; second, the algorithm speed can be increased significantly with a minimal reduction in accuracy. The versatility of the algorithm has been tested using both near infrared iris images acquired with a hand-held device and colour iris images acquired in unconstrained environment.

1 Introduction

The iris was shown to be a strong biometric modality, remaining stable over many decades. Iris Recognition systems with high accuracy have been built [Da04] since the early 90's. Although high accuracy can be obtained using iris biometrics, there are no implementations yet on common portable devices, such as laptops or cellphones, mainly because of the constraints required for the capture and recognition process. Generally, these constraints refer to the need for near infra red illumination and the high degree of cooperation from the user. Usually the user is asked to stay very close to the acquisition device, to align his eyes with the device and to stand still for a few moments.

An Iris Recognition system may be considered as consisting of five main stages: acquisition, segmentation, normalization, feature extraction and classification or matching. In the recent past, several iris recognition techniques have been proposed [Ma06], where the distance between the user and the device may exceed 1 meter and the degree of cooperation from the user does not have to be large. At present, the research in iris recognition is focused on non-cooperative and unconstrained operations of these biometric systems. In such systems, the 'segmentation' stage of iris recognition plays a vital role because feature extraction from non-iris texture will be useless.

Iris recognition from hand-held devices, where the device could have near infra red illumination or on wall-mounted devices, where the user is semi-cooperative can be considered unconstrained. In this paper we present a novel iris segmentation algorithm that is able to work in both near infra red and visible spectrum with good performance. As far as we know, this is one of the first iris segmentation algorithms capable of achieving acceptable accuracy in both wavelengths spectrums. The difficulty with which a segmentation algorithm performs well in different spectrums is mentioned in [PA05], where the UBIRISv1 [PA04], a colour iris image database is presented. The authors of [PA05] have implemented several iris segmentation techniques and tested them on UBIRISv1 database and on CASIA v1 database [In04], which has near infra red iris images. They observed and reported numerically that the algorithms were performing well either on visible spectrum or on near infrared iris images, but not on both wavelength domains. The importance of a segmentation algorithm performing acceptably on both kinds of data consists in making the iris detector adaptable for different types of iris recognition systems deployed either in a constrained environment or in a more non-cooperative scenario.

A second contribution of this paper is the speed at which this algorithm is capable of roughly segmenting both the iris and the pupil. With only approximately 3% reduction accuracy comparing to normal operation, the proposed algorithm is capable to segment 2 images per second when running on an entry-level computer, i.e. single core processor with 2-4 GB of RAM. This processing time places the proposed method among the fastest iris segmentation algorithms available in the literature for colour iris images.

To encourage the efforts of researchers in segmenting noisy iris images, acquired in less constrained environment and visible light, a worldwide competition has been organized. This competition was called Noisy Iris Challenge Evaluation (NICE) [PA07] and it took place in 2 parts: Part 1 assessed only the segmentation of a subset of UBIRISv2 [Pr10] and Part 2 the classification algorithms were assessed on the same images. The winning algorithm for segmentation is depicted in [THS10] and for part 2 the algorithms will be published soon.

Among the iris segmentation algorithms that have been reported the most popular is the integro-differential operator used in [Da04], which is being implemented on the most of the commercial iris recognition systems. Another well-known iris detection method is described in [Wi97], where Canny edge detector and Hough Transform were used in a 2 steps approach. Inspired by the principle of the integro-differential operator, new operators have been developed for iris segmentation in [CW04], [MSS02] and [Tu94].

In the literature, usually an iris segmentation algorithm is said to be robust if its performance does not decrease as the noise and distortions in the images is increased [PA06]. However, the term robust is wider for an iris segmentation method. For example, the robustness could include the versatility of the algorithm in segmenting both near infra red and colour iris images with comparable accuracy. Moreover, the segmentation algorithm is robust if it can be adapted to improve its throughput with a minimal reduction in accuracy. The method described in this paper was designed according to this extended definition for the robustness of a segmentation algorithm.

The remainder of this paper is organized as follows: in section 2 the details of iris and pupil segmentation are given. In section 3 an enhancement to the pupil segmentation is described and in section 4 the experimental results are reported. Conclusions are given in section 5.

2 Proposed Segmentation Algorithm

Both the iris and pupil have approximately the shape of a circle if the image of the eye does not include strong off-angle deformation. Therefore a circle detection method could be used to segment the iris and pupil. According to [Da04] the minimum radius of the iris has to be 70 pixels, so that the iris texture from the image is useful for recognition. The iris image dimensions should, therefore, be high enough to include an iris diameter of at least 140 pixels, but if they are very large, then the possible iris radius will lie in a range from 70 to a high value. This will make the segmentation process very time consuming. To avoid such situation, circle detection algorithms are usually provided as parameters the upper and lower limits of the radius of the iris and the pupil. For a certain dataset, these limits are known. The algorithm depicted in this paper uses the same approach.

The iris segmentation method proposed in this paper is able to work both on near infra red images and colour images with similar performance. The segmentation of the iris and pupil described in this section will be exemplified on colour images from UBIRISv1 dataset [PA04]. For a better understanding, a block diagram of the system is presented in Figure 1.

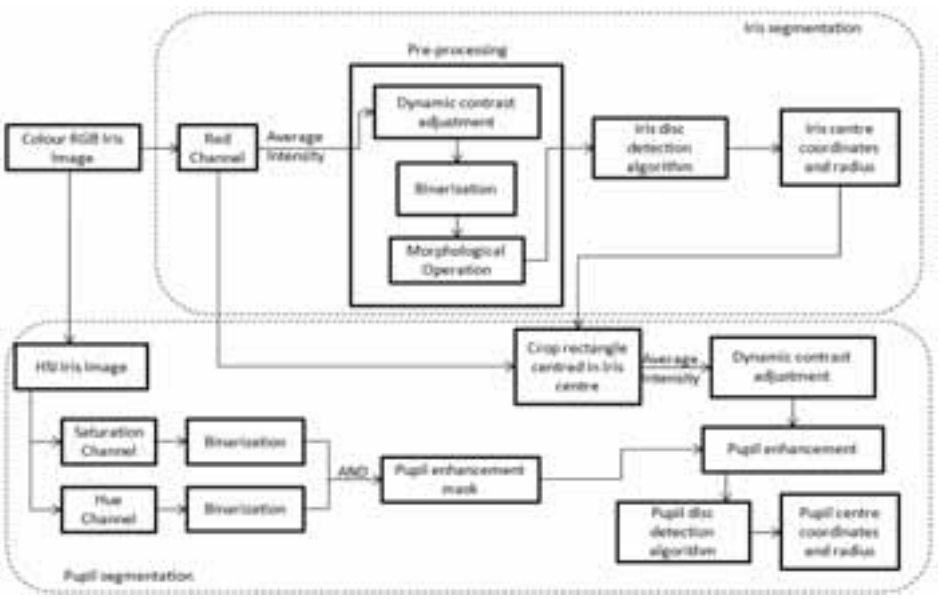

Figure 1: Block diagram of the segmentation algorithm

2.1 Iris Detection

In an un-constrained environment, where near infra red illumination is not possible, only visible spectrum (e.g. colour RGB) iris images are available. For iris segmentation we have used only the red channel. To cope with illumination variations of the iris image, a dynamic contrast adjustment was made. The adjustment parameters depend on the average intensity of all pixels from the red channel iris image. The image was then binarized using a threshold depending on the average intensity of all pixels. The effects of these transformations are shown in Figure 2. After binarization, a spur morphological transformation has been applied to the image in order to eliminate the isolated white pixels from the iris region and black pixels in the sclera.

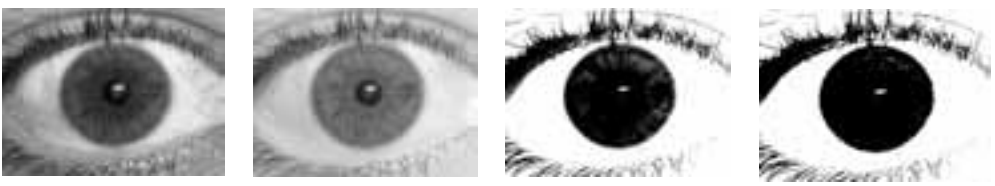

a) b) c) d)

Figure 2: Iris image transformations: a) original RGB image from UBIRISv1 dataset; b) red channel image; c) image after contrast adjustment; d) binarized iris image.

Now the iris is a black circular disc and clearly separated from the rest of the image. To determine accurately where the centre is and the corresponding radius, a simple geometrically-based method is used. Any pixel within the rectangle obtained by subtracting the minimum iris radius from each side of the image is considered a potential candidate to the centre of the iris. The reduced search space was chosen such as the iris is not partially out of the image and for increased speed. The centre of the iris is insured to be inside the rectangle. Still, this approach enables the method to detect the iris even if it is not centred or the user is looking to the left or right.

The underlying principle behind the proposed segmentation algorithm is a simple one: the distances from the centre of the iris to its boundary should be equal. Each pixel within the isolated rectangle is considered the intersection point of 3 lines at predefined slopes. One line was drawn out in the horizontal direction and the other two were symmetric to the first line, as shown in Figure 3. For each pixel that is the intersection of 3 lines, 6 line segments are scanned along, starting at a distance from the maximum iris radius to the minimal iris radius, measured from the intersection. The scanning directions are from the end points of the lines towards the intersecting pixel. Then the Euclidean distances are computed from the white to black transition to the intersecting pixel. The transition from white to black along a line segment is considered to be the transition from the longest white segment to black, when scanning towards the intersection pixel. In total there are 6 distances. To speed up the segmentation process, the original image is downsized by a factor of 4.

In our implementation, the slopes of the line segments used are within ± 30^o about the horizontal. The slopes were chosen so that occlusions from the top and bottom of the iris are avoided. Exact slopes of the lines are not very important and small variations do not have any significant effect on the performance of the algorithm.

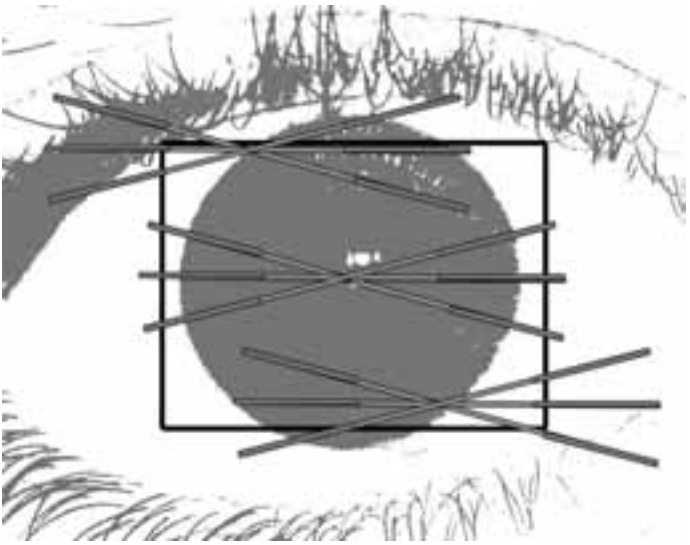

Figure 3: Potential iris centre locations are the intersection of 3 lines

After obtaining the 6 distances, the centre of the iris is assigned to the pixel which is located at an approximately equal distance from all the 6 white to black transitions. If we denote the 6 distances with $dist_i$, where i=1,...,6, and (k, l) ϵ S, where S is the reduced search space, the coordinates of the iris centre (i_r, i_c) are chosen according to equation (1).

$$(\mathbf{i_r}, \mathbf{i_c}) = \arg \min_{\forall (\mathbf{k},\mathbf{l}) \epsilon \mathbf{S}} \left[\frac{\left[\left(\sum_{i=1}^{5} \sum_{j=i+1}^{6} \left| \mathbf{dist_j} - \mathbf{dist_i} \right| \right) \right]}{\mathbf{15}} \right] \quad (1)$$

The iris radius *irisRad* is obtained with the following equation, considering that the 6 distances correspond to the pixel found with equation (1):

$$irisRad = \frac{1}{6} \sum_{i=1}^{6} \mathbf{dist_i} \quad (2)$$

The rationale behind having 3 lines, respectively 6 segments is to avoid confusing the algorithm when black isolated regions are located in the sclera. If only 2 lines are considered and some isolated black pixels are in the sclera, the method will incorrectly detect the iris. Other variations of this method could be obtained by enlarging the number of lines and segments to be scanned. When speed is not essential, more than 3 lines could be considered to improve the segmentation accuracy. Also, the speed may be increased by enhancing the search method for the centre pixel. If only the black pixels are considered in the algorithm, the number of pixels that are potential centres of the iris is significantly reduced. Another way of reducing the search space is to consider every other pixel instead of repeating the process for all the pixels within the rectangle. Time execution could be also reduced by starting with the pixels from the centre of the rectangle and stop when it is observed that the value returned by (1) is increasing repeatedly for the following pixels.

2.2 Pupil Detection

When acquiring iris images in the near infrared spectrum, the pupil's colour is almost black and it is very easy to segment if there are no occlusions present. This is due mainly to the fact that under near infrared lighting, specular and difuse reflections are normally not present in the image. The reflections are not captured under near infrared illumination because of melanin pigment present in the iris, which is not visible in near infrared spectrum. For iris images captured under visible wavelength the boundary between the pupil and the iris is less distinguishable than in near infrared and moreover, the pupil becomes more difficult to segment because of the reflections that are present in the image. Therefore, a segmentation method designed for near infra red iris images is likely to perform worse on visible wavelength images and vice versa.

Usually, in colour iris images a specular reflection is present in the pupil or at the boundary between the pupil and the iris. The algorithm uses only the region from the image that is inside the detected iris. In this way we ensure that the pupil will not be detected outside the iris. We employed as a first step a threshold-based technique that is used to detect specular reflections inside the iris. After the specular reflections have been detected, the average of the intensity of the remaining pixels from inside the iris was calculated. This average value was then used to dynamically adjust the parameters of a contrast adjustment operation, as described in subsection 2.1. The parameters were obtained empirically. Bearing in mind that the iris and pupil are not concentric but their centres are located close one to each other, the search area for the pupil centre can be significantly reduced. A rectangular region of interest is formed having the centre of mass the centre of the iris and the width and length obtained with Equation (3). The parameters in equation (3) have been obtained experimentally. The results of these steps are shown in Figure 4.

$$\begin{cases} length = irisRad * 0.4 \\ width = irisRad * 0.25 \end{cases} \quad (3)$$

where *irisRad* is the radius of the detected iris.

a) b)

Figure 4: Pupil segmentation: a) cropped iris image from red channel; b) iris after contrast adjustment and the rectangle containing the pupil's centre.

This considerably speeds up the pupil segmentation process. The problem that may occur using this approach is when the iris is not correctly located. If the iris is not correctly roughly segmented, the pupil segmentation will not be successful, as our algorithm will try to locate the pupil only inside the iris. This will rarely happen, since the method proposed for iris detection yields a very high accuracy in roughly locating the iris, i.e. over 99%, as reported in experimental results section.

It can be observed from Figure 4 that after contrast adjustment the pupil became very well separated from the iris texture. For segmenting the pupil, we consider all the pixels inside the rectangle defined with (3) as possible centres of the pupil. Each of these pixels is considered the centre of two concentric circles, one with a radius smaller with two pixels than the other. The 2 circles will have a radius ranging from the minimum to the maximum possible pupil radius. Figure 5 illustrates this scheme. For each pair of circles, the difference between the values of the pixel intensities of the larger circle and the pixels of the smaller circle is computed. To speed up the process, only 30 corresponding pixel positions along the arcs of the circles are considered, i.e. with a step of 12 degrees.

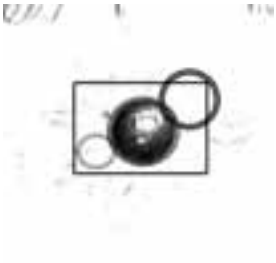

Figure 5: Pairs of concentric circles used for pupil segmentation.

For each pair of circles there are 30 differences. Let these be denoted by $diff_i$, where

i=1,...,30 and the centre of the pupil be (c_r, c_c). If r_{min} and r_{max} are the minimum and maximum possible radiuses of the pupil, (k, l) ϵ S and S is the area defined by (3), the coordinates of the centre of the pupil will then be determined according to equation (4).

$$(\mathbf{c_r}, \mathbf{c_c}) = \arg \max_{\forall (\mathbf{k},\mathbf{l}) \epsilon \mathbf{S}} \left(\max_{\mathbf{r_{min}} < r < \mathbf{r_{max}}} \sum_{\mathbf{i=1}}^{\mathbf{30}} \mathbf{diff_i} \right) \quad (4)$$

The rationale behind this approach is to maximize the sum of differences of pixels intensities, between pixels that are positioned on two concentric circles. The centre of the circles with the maximum difference will be the pupil's centre.

2.3 Near infrared operation

The operation of the proposed algorithm in near infra red domain is slightly different than that in colour domain. First, the pupil is detected in a near infra red iris image, not the iris, as in colour images, because the pupil in near infra red spectrum is very dark and easy to segment. The interesting thing is that the method described in section 2.1 for iris segmentation is used for pupil segmentation in near infra red images and the method described for pupil segmentation in Section 2.2 is used for iris segmentation.

For pupil detection, a simple contrast adjustment operation is sufficient to leave only the pupil and eyelids and eyelashes in the image. The region of interest for pupil is restricted to a rectangle obtained by subtracting the minimum iris radius from each side of the image. Then, the method described in subsection 2.1 is applied to find the pupil.

After finding the pupil's centre and radius, the search space for iris centre will be reduced only to the pixels inside the detected pupil. Those pixels will become the centres of the two concentric circles and the iris-sclera boundary is found by applying equation (4). Based on the image, the correct mode (color or infrared) is chosen by the algorithm.

3 Pupil Segmentation Enhancement

For further improving the segmentation algorithm, some additional operations were incorporated to cope with more 'difficult to segment' iris images. In visible spectrum some iris images are captured under poor illumination and the boundary between the iris and the pupil are almost unnoticeable. Also strong reflections could have the similar effect. An iris image from UBIRISv1 dataset, Session 2, affected by these types of noises is shown in Figure 6a.

a) b)

Figure 6: a) Noisy iris image, where the iris-pupil boundary is difficult to distinguish; b) Contrast adjustment for pupil detection in noisy iris images

As noticeable from Figure 6a, the intensity values of the pixels inside the pupil are not very different from those belonging to the iris texture. This fact will make the contrast adjustment operation not so effective in highlighting the pupil as it was before. The effect of the contrast adjustment for pupil detection for the image from Figure 6a is shown in Figure 6b.

To make the algorithm robust to imperfections such as noise and occlusions, especially to images captured under poor illumination, we propose an enhancement based on other colour spaces than RGB. When converting from RGB colour space to HSI, we observed that in hue and in saturation channels, the area pf the pupil from the original RGB image is clearly distinguishable. The gray-scale images of hue channels of the same image from Figure 6a is shown in Figure 7a.

a) b)

Figure 7: a) Iris image in hue channel; b) Contrast adjustment augmented with information from HSI colour space for pupil segmentation

The hue channel has also been used for pupil segmentation in [PA06] and in [FC10], but in the present algorithm we use the information from saturation channel also. Empirically observing that the pupil in the hue channel has values between 130 and 170 and in the saturation channel has values between 70 and 130, we created a binary mask of the pupil from both hue and saturation channels. A combined mask for the pupil was obtained by AND operation of the 2 masks. The combined mask was used then to assign to the corresponding pixels from the red channel a low value. The contrast adjusting from Figure 6b was complemented with the information from hue and saturation channels, yielding the images shown in Figure 7b. Using the information from HSI colour space, the pupil becomes visibly easier to segment.

4 Experimental Results

4.1 Databases

The robustness of the proposed segmentation algorithm was assessed by using it to segment both near infra red and colour images. The near infra red dataset used in our experiments is CASIAv3 [In06], the Lamp subset, which has 16213 images from 411 users. The images were acquired using a hand-held device with a lamp turned on and off to make the pupil to dilate. We ran the experiments on CASIAv1 [In04] also, for comparison with other reported accuracies.

The second database used in our experiments is UBIRISv1 [PA04]. This database consists of 1877 800x600 pixles, colour RGB images collected from 241 individuals in 2 sessions. The enrollment has been made using only the right eye with 5 images for each user. In the first session the images are captured in a constrained environment, with minimized noise factors. In the second session the environment is one with reduced constraints and noise factors are present in the images, such as reflections, luminosity variations and poor focus. In the first session, all 241 users have been enrolled, resulting in a total of 1205 images, while in the second session, only 132 users out of the 241 are enrolled.

4.2 Results

The proposed algorithm was implemented in Matlab environment. The machine used to run the experiments had an Intel Core 2 Duo processor running at a frequency of 2.4 GHz and 4 GB of RAM. In order to be able to compare our results with other published segmentation algorithms in terms of speed, only one core of the Intel processor has been used.

The assesment of the algorithm was done by visually inspecting the segmented images. The images have been reduced in size by a factor of 4 to increase the speed of the algorithm. One iris image is considered correctly segmented if both the iris and the pupil were segmented correctly, i.e. the circles are falling exactly on the edges of the iris and pupil. For CASIA v3 dataset, Lamp subset, the obtained segmentation accuracy is 92.04%. The pupil segmentation accuracy is 98.15%.

For UBIRISv1 the segmentation accuracies for both Session 1 and 2 are comparable with other reported results in the literature. For Session 1 we obtained 95.46% accuracy and for Session 2 we obtained 87.03%. In [PA05] the authors have implemented a number of iris segmentation algorithms to compare with their own. In Table 1 we present their best 2 reported segmentation accuracies for the most popular algorithms for UBIRISv1 and CASIAv1 datasets. The table shows that the algorithms are not performing well on both near infrared images and colour images, while the proposed algorithm does. The execution time for our algorithm is aproximately 2.97 seconds. This time is comparable to the execution time needed by Daugman's integro-differential operator, which implementation we ran in aproximately 2.6 seconds.

Methodology	UBIRISv1	CASIAv1
Daugman [Da04]	93.53 %	54.44 %
Wildes [Wi97]	89.12 %	84.27 %
Proposed Methodology	92.46 %	91.97 %

Table 1: Iris segmentation algorithms accuracies

Usually, segmentation is the most time consuming of all the stages in an Iris Recognition system. The algorithm proposed in this paper can be adapted to work a faster with a minimal reduction in accuracy by resizing the iris image. For iris boundary detection, the image is reduced in size by a factor of 10 for UBIRIS v1 dataset, and for pupil segmentation, the image is downsized 6 times.

In iris recognition the part of the iris texture that is closer to the pupil is richer and less redundant in radial direction than the texture close to the outter boundary [Da04]. Therefore, the efforts in detecting very accurately the iris-sclera boundary could be minimized by detecting it less accurately when speed is a critical requirement of the application. When resizing an iris image 10 times, the proposed algorithm detects the outer iris boundary in the smaller image, but when the circle coordinates are multiplied by 10 to get to the original size, some of the circles do not fit exactly the outer iris boundary. However, in pupil segmentation, the downsizing factor used was 6, as the pupil segmentation accuracy is much more important in extracting useful features. In this size reduction, the pupilary boundary can still be detected very accurately in most of UBIRIS v1 images with original resolution 800 by 600 pixels.

After these modifications, the accuracy obtained for session 1 is 92.36% and for session 2 is 83.96%, with an average segmentation time of only 0.48 seconds. Therefore, with approximately only 3% decrease of accuracy, the segmentation algorithm is almost 6 times faster, being suitable for realistic scenarios implementations.

5 Conclusions

Research in Iris Recognition is focusing more and more on unconstrained and non-cooperative operation of these type of biometric systems. The noisy iris images coming from an unconstrained environment are often difficult to segment and match. The need for robust and fast segmentation algorithms determined the research community to develop new methods to segment noisy iris images.

This paper proposes a novel iris segmentation method which is able to cope with noisy images from both visible and near infra red spectrum with good performance. The segmentation accuracies obtained are similar for the two wavelength domains. For iris detection, the red channel was used in colour images. For pupil detection, the same red channel of the original colour image is used, with additional information from hue and saturation channels of HSI colour space. By resizing the image, the algorithm performs a few times faster with a minimal reduction in accuracy. This makes the proposed algorithm a good choice for embedded or hand-held devices. Experimental results on UBIRIS v1 and CASIA v3 datasets prove the versatility of this algorithm. The methods for iris and pupil detection could be also used as generic circle detection methods.

Acknowledgment

This work is part of the NOmad Biometric Authentication (NOBA) project funded by ERDF under the Interreg IVA program (Ref. No. 4051) in collaboration with ESIGELEC/IRSEEM.

References

[CW04] Camus, T. A.; Wildes, R. P.: Reliable and fast eye finding in close-up images. IEEE 16th International Conference on Pattern Recognition, Quebec, Canada, 2004, pp. 389 – 394.

[Da04] Daugman, J.: How Iris Recognition Works. IEEE Transactions on Circuits and Systems for Video Technology, vol 14, 2004, pp. 21-30.

[FC10] Filho, C. F. F. C.; Costa, M. G. F.: Iris segmentation exploring colour spaces. Image and Signal Processing (CISP) 2010, 3rd International Congress on, pp: 1878 – 1882.

[In04] Inst. of Automation, Chinese Academy of Sciences: CASIA Iris Image Database. http://www.idealtest.org/dbDetailForUser.do?id=1, May 2011.

[In06] Inst. of Automation, Chinese Academy of Sciences: CASIA Iris Image Database Version 3.0. http://www.idealtest.org/dbDetailForUser.do?id=3, May 2011.

[Ma06] Matey, J.R.; Naroditsky, O.; Hanna, K.; Kolczynski, R.; Lolacono, D. J.; Mangru, S.; Tinker, M.; Zappia, T. M.; Zhao, W.Y.: Iris on the Move: Acquisition of Images for Iris Recognition in Less Constrained Environments. Proceedings of IEEE, vol. 94, 2006, pp. 1936-1947.

[MSS02] Martin-Roche, D., Sanchez-Avila, C., Sanchez-Reillo, R.: Iris recognition for biometric identification using dyadic wavelet transform zero-crossing. IEEE Aerosp. Electron. Syst. Mag., 2002, 17(10), pp. 3–6.

[PA04] Proenca, H.; Alexandre, L. A.: UBIRIS Iris Image Database. http://iris.di.ubi.pl, May 2011.

[PA05] Proenca, H.; Alexandre, L. A.: UBIRIS: A Noisy Iris Image Database.

[PA06] Proenca, H.; Alexandre, L. A.: Iris segmentation methodology for non-cooperative recognition. Vision, Image and Signal Processing, IEE Proceedings, vol 153, 2006, pp. 199-205.

[PA07] Proenca, H.; Alexandre, L. A.: Noisy Iris Challenge Evaluation – Part I. http://nice1.di.ubi.pt/index.html, May 2011.

[Pr10] Proenca, H.; Filipe S.; Santos, R.; Oliveira, J.; Alexandre, L.A.: A Database of Visible Wavelength Iris Images Captured On-the-Move and At-a-Distance. IEEE Transactions on Pattern Analysis and Machine Intelligence, vol 32, 2010, pp. 1529 – 1535.

[THS10] Tan, T.; He, Z.; Sun, Z.: Efficient and robust segmentation of noisy iris images for non-cooperative iris recognition. Image and Vision Computing, vol. 28, 2010, pp. 223 – 230.
[Tu94] Tuceryan, M.: Moment based texture segmentation. Pattern Recognition Letters, 1994, v.15, pp. 659–668.
[Wi97] Wildes, R. P.: Iris Recognition: an emerging biometric technology. Proceedings of IEEE, vol. 85 (9), 1997, pp. 1348 – 1363.